

# Nodal Superconductivity with Multiple Gaps in $\text{SmFeAsO}_{0.9}\text{F}_{0.1}$

Yonglei Wang, Lei Shan,\* Lei Fang, Peng Cheng, Cong Ren, and Hai-Hu Wen†

National Laboratory for Superconductivity, Institute of Physics & Beijing National Laboratory for Condensed Matter Physics, Chinese Academy of Sciences, P.O. Box 603, Beijing 100190, China

(Dated: March 15, 2019)

We report the observation of two gaps in the superconductor  $\text{SmFeAsO}_{0.9}\text{F}_{0.1}$  (F-SmFeAsO) with  $T_c = 51.5\text{K}$  as measured by point-contact spectroscopy. Both gaps decrease with temperature and vanish at  $T_c$  and the temperature dependence of the gaps are described by the theoretical prediction of the Bardeen-Cooper-Schrieffer (BCS) theory. A zero-bias conductance peak (ZBCP) was observed, indicating the presence of Andreev bound states at the surface of F-SmFeAsO. Our results strongly suggest an unconventional nodal superconductivity with multiple gaps in F-SmFeAsO.

PACS numbers: 74.20.Rp, 74.45.+c, 74.50.+r

Recently, superconductivity was discovered in Fe-based layered superconductor  $\text{LaFeAs}[\text{O}_{1-x}\text{F}_x]$  (F-LaFeAsO) [1]. By replacing La by some other rare earth elements,  $T_c$  was improved quickly up to 55K [2] which is substantially higher than that of the single-layered cuprate superconductors and exceeds the theoretical value predicted by the conventional BCS theory [3]. The superconductivity was also observed in hole doped case [4, 5]. Thus a new family of high- $T_c$  superconductors was opened up, providing an unique chance to understand high- $T_c$  superconductivity. To detect the gap structure and pairing symmetry is an essential step to reveal the mechanism of these Fe-based superconductors. The specific heat measurement on F-LaFeAsO showed a nonlinear magnetic field dependence of the electronic specific heat coefficient as expected by a nodal superconductor [6]. This was proved subsequently by the measurements of point-contact spectroscopy [7], lower critical field  $H_{c1}$  [8], London penetration depth  $\lambda$  and spin-lattice relaxation rate  $1/T_1$  [9, 10]. The muon spin relaxation measurements also presented the possibility of dirty  $d$ -wave pairing [11]. Theoretically, some calculations support  $d$ -wave [12, 13, 14] while others support an unconventional  $s$ -wave pairing [15, 16]. Most surprisingly, recent Andreev reflection data favor an isotropic single gap in  $\text{SmFeAsO}_{0.85}\text{F}_{0.15}$  and  $\text{NdFeAsO}_{0.85}$  [17, 18], while a nodal superconductivity with two-gap structure was suggested by the NMR experiment on  $\text{PrFeAsO}_{0.89}\text{F}_{0.11}$  [19]. Actually, multi-band superconductivity has been predicted theoretically [12, 20, 21, 22, 23] and was supported by the magnetic properties of  $\text{SmFeAsO}_{0.8}\text{F}_{0.2}$  single crystal [24] and the high-magnetic field resistance of  $\text{LaFeAsO}_{0.89}\text{F}_{0.11}$  [25]. However, multiple gaps have not been detected for the moment by both Andreev reflection or tunneling experiment which is a powerful tool to measure the superconducting gap. Therefore, more experiments on the samples with higher quality are strongly desired.

In this paper, we present the point-contact spectroscopy data of the compact and rigid  $\text{SmFeAsO}_{0.9}\text{F}_{0.1}$  (F-SmFeAsO) samples. A ZBCP was observed repeat-

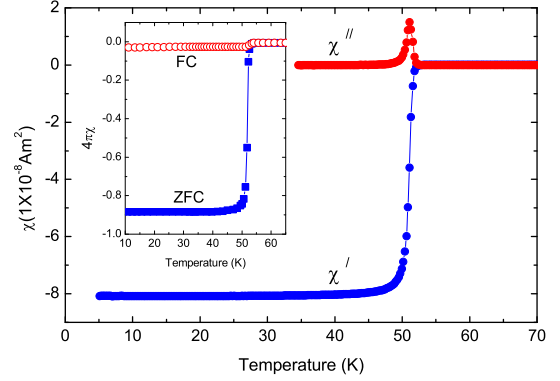


FIG. 1: (Color online) Temperature dependence of AC susceptibility of F-SmFeAsO. Inset: DC susceptibility of F-SmFeAsO.

edly, indicating the nodal gap structure of F-SmFeAsO similar to that of F-LaFeAsO. Moreover, two different gaps were observed and both of them decrease with temperature and vanish at  $T_c$ . These results strongly suggest that F-SmFeAsO has an unconventional nodal superconductivity with multiple gaps.

The superconducting F-SmFeAsO samples were prepared by a high pressure synthesis method [26]. The detailed information about the synthesization is elaborated in a recent paper [2]. As shown in Fig. 1, DC susceptibility (measured under a magnetic field of 1 Oe) and AC susceptibility data (measured using an AC amplitude of 0.1 Oe) exhibit a sharp magnetic transition. The width defined between the 10% and 90% cuts of the transition is below 2K, with the middle of the Meissner transition at 51.5 K, indicating the good quality of the superconducting phase. Compared with the samples synthesized by the common vacuum quartz tube synthesis method, the samples studied here are much more compact and rigid, thus more suitable for point-contact spectroscopy measurements. The point-contact junctions are prepared by carefully driving the Pt/Ir alloy or Au tips towards the sample surface which is polished and cleaned beforehand.

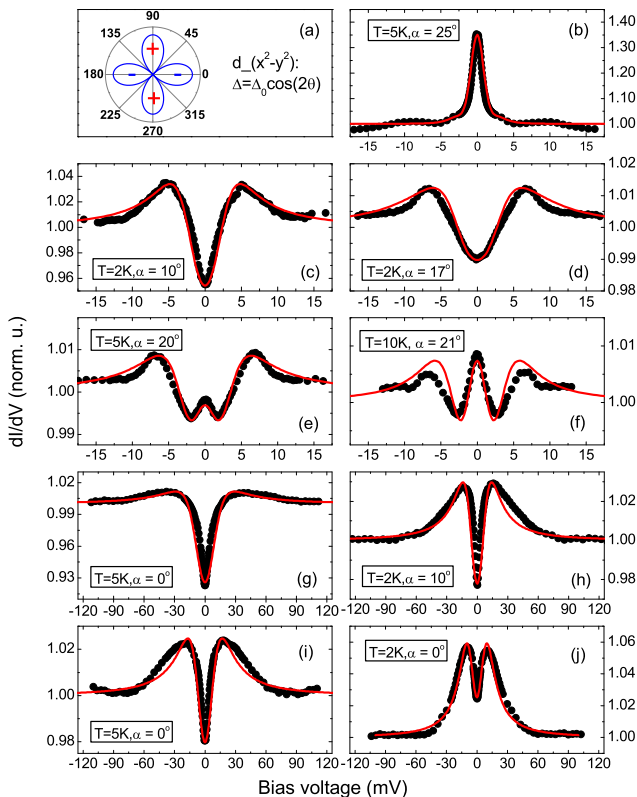


FIG. 2: (Color online) (a) Gap structure (d-wave type) used to fit the experimental data. (b)-(j) Experimental data (solid circles) measured at various locations on the sample surface and theoretical calculations (solid lines) with the gap function shown in (a).

The tip's preparation and the details of the experimental setup were described elsewhere [27]. Typical four-terminal and lock-in techniques were used to measure the conductance-voltage ( $dI/dV - V$  or  $G - V$ ) characteristics. Each measurement is comprised of two successive cycles, to check the absence of heating-hysteresis effects.

Figure 2 shows the  $G - V$  curves measured at various locations on the sample surface, which have been normalized by the high-bias data. A distinct ZBCP can be seen in Figs. 2(b),(e) and (f), indicating the existence of surface Andreev bound states, which is a clear signature of the pair potentials with reversal sign in momentum space and is known as a unique character of nodal superconductors [28]. Such ZBCP has also been observed in F-LaFeAsO [7] and F-NdFeAsO, thus nodal superconductivity is most possibly a common property of the Fe-based superconductors. Blonder *et al.* [29] have proposed a simplified theory for the  $G - V$  curves of an  $s$ -wave superconductor/normal metal junction separated by a barrier of arbitrary strength. The barrier strength is parametrized by a dimensionless number  $Z$  which describes the crossover from metallic to ideal tunnel junction behavior by  $Z = 0$  to  $Z = \infty$ . Obviously, this  $s$ -wave

model can not explain the observed ZBCP. Tanaka and Kashiwaya [30] extended the BTK model to deal with the issue of unconventional pairing symmetry. In this case, the angle ( $\alpha$ ) between the quasiparticle injecting direction and the main crystalline axis was introduced as another parameter. Moreover, the isotropic superconducting gap  $\Delta$  was replaced by an anisotropic gap with  $d_{x^2-y^2}$  symmetry:  $\Delta = \Delta_0 \cos(2\theta)$ , as shown in Fig. 2(a). It was then predicted that, for  $Z > 0$  the ZBCP is formed for all directions in the  $a - b$  plane except when tunneling into the (100) and (010) planes. This ZBCP will be suppressed when the quasiparticle scattering is strong enough [31]. It was found that all the spectra shown in Fig. 2 can be described very well by this extended BTK model. Moreover, various quasiparticle injecting angles ( $\alpha$ ) are obtained for the spectra measured at different positions, indicating that our measurement is a local detection. The broadening parameter  $\Gamma/\Delta_0$  [32] in the calculations is between 0.2 and 1, coming from some unclear scattering mechanisms at the interface, which is similar to the case of cuprate superconductors. It should be mentioned that the gap structure with reversal sign is necessary to explain our data while the details of the gap function can not be distinguished although the  $d_{x^2-y^2}$ -wave symmetry was accepted here.

Another remarkable find in the calculations presented in Fig. 2 is that, the determined maximum gap  $\Delta_0$  can be divided into two groups, namely, a big gap of  $10.5 \pm 0.5$  meV and a small gap of  $3.7 \pm 0.4$  meV, though the barrier strength  $Z$  and quasiparticle injecting angle  $\alpha$  are random due to the diverse configuration of the grains in the polycrystalline samples. The small gap can not be explained as degradation of the sample surface since its value is distributed in a narrow range far below that of the big gap. To our knowledge, this multi-gap feature is observed for the first time in transition metal-based high- $T_c$  superconductors. To get further insight into this point, we have measured the temperature dependence of these two gaps with distinct energy scales.

Figure 3 shows the temperature dependence of two types of spectra corresponding two different gaps as mentioned above. At lower temperatures, two coherence peaks can be seen clearly accompanied by low-energy depression of the quasiparticle density of states. With increasing temperature, the peaks are suppressed and smeared continuously and finally the spectra become a smooth featureless curve around  $T_c$ . These data were normalized (by the data of  $T = 60K$ ) in order to be compared with theoretical models, as shown in Figs. 4(a) and (b). It was found that all the data can be fitted very well to the extended BTK model mentioned above. Fig. 4(c) shows two spectra measured at the same location while with different junction resistances and hence different barrier strengths. The similar gap value about 10 meV was obtained from these spectra, indicating that the detected superconductivity does not depend on the

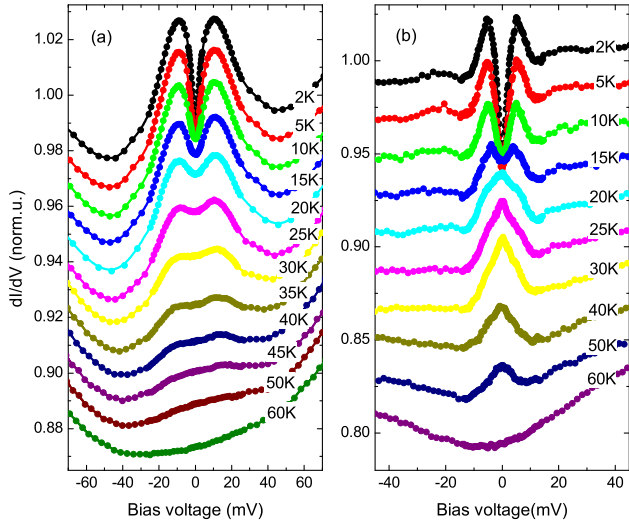


FIG. 3: (Color online) Conductance measured for various temperatures from 2K to above  $T_c$ . (a) large gap, (b) small gap. All the curves except the top one are offset downwards for clarity.

junction resistance. Fig. 4(d) summarizes the gap values obtained from Figs. 4(a) and (b). The temperature dependence of both the large gap and the small one can be described by the prediction of BCS theory. The gap value of  $\Delta_0 = 10\text{meV}$  leads to  $\Delta_0/k_B T_c = 2.3$ , a bit larger than the prediction of weak-coupling  $d$ -wave BCS theory. Moreover, both gaps are closed around  $T_c$  reflecting the inter-band coupling existing in this material.

It is interesting to note that some spectra exhibit a two-gap feature similar to that of  $\text{MgB}_2$ . As shown in Fig. 4(e), compared with the high-temperature spectrum measured around  $T_c$ , the low-temperature one has three distinct features: a ZBCP, two coherence peaks, and two symmetric hump at higher energy. In Fig. 4(f), we try to simulate the low-temperature spectrum after normalization according to the high-temperature one. In the calculation, a simple two-component BTK model was accepted in which the normalized conductance ( $G = dI/dV$ ) is expressed by  $G = w_1 G_1 + w_2 G_2$ , where  $G_1$  and  $G_2$  are the conductance associated with the large gap and small gap, respectively,  $w_1$  and  $w_2$  ( $w_1 + w_2 = 1$ ) are corresponding weights of these two gaps contributing to the total conductance. In order to reduce the number of fitting parameters, the  $s$ -wave symmetry was assumed for the large gap while the  $d_{x^2-y^2}$ -wave symmetry for the small gap. It was found that the main features in the spectrum can be fitted very well. Although this is a rough approximation, it captures the main physics of multiple gaps and nodal superconductivity. Most interestingly, the determined gap values from the calculation are 11meV and 4.5meV, very close to the results obtained from the spectra measured at other locations.

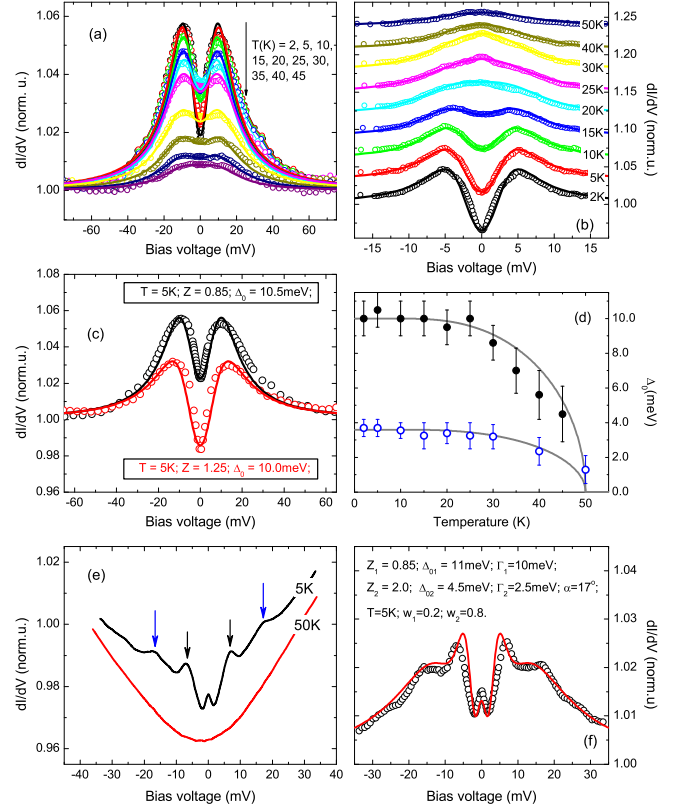


FIG. 4: (Color online) (a) and (b) Temperature dependence of normalized spectra corresponding to Figs. 2(a) and (b), respectively. The solid lines are theoretical calculations according to the extended BTK model. (c) Two spectra measured at same position while with different junction resistance, solid lines are theoretical calculations. (d) Temperature dependencies of the gap values determined from fits as shown in (a) and (b), solid lines are the prediction of BCS theory. (e) The spectra measured at low temperature and around  $T_c$  on same position of the sample surface. (f) The low-temperature spectra after normalization according to the high-temperature one as shown in (e), the solid line is the theoretical fit.

Besides the sample of  $\text{F-SmFeAsO}$  which is focused on in this work, we have also measured the point-contact spectra of  $\text{F-LaFeAsO}$  [7] and  $\text{F-NdFeAsO}$ . In those samples, a more prominent ZBCP was often observed while some confused backgrounds can also be observed occasionally compared with the data of  $\text{F-SmFeAsO}$ , thus quantitative analysis is more difficult. A most possible explanation for this difference is that,  $\text{F-SmFeAsO}$  studied here was prepared by high-pressure technique while other samples were synthesized in atmospheric pressure and hence more fragile and loose. Therefore, there is often a space between adjacent grains, which can be seen clearly in the SEM photographs. Consequently, the tip is easy to penetrate through the sample surface and rests on a pit, leading to multiple contacts between the tip and surrounded micro-crystals. On the one hand, it increases

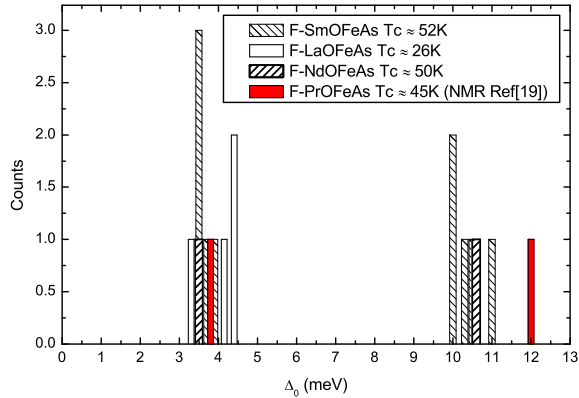


FIG. 5: (Color online) Statistical chart of the  $\Delta_0$ -values determined from the spectra measured at various positions on the sample surfaces. The vertical axis denotes the occurring times for a given gap-value specified by the horizontal-axis.

the opportunities to detect strong ZBCP if a nodal pairing symmetry exists. On the other hand, it will induce a more confused background due to the complicated interface effect. In this case, the gap values can still be estimated by using a convenient method proposed by Dagan *et al.* [33]. The method of data analysis consists simply in subtracting conductances measured in an applied field from the zero field conductance. Since the maximum of the density of states at the gap value should be sensitive to an applied field, such subtraction will lead to a dip around the gap value in the subtracted spectra [33]. Using this method, we have estimated  $\Delta_0 \approx 3.9\text{meV}$  for F-LaFeAsO, which is consistent with the results from both specific heat [6] and lower critical field [8].

In Fig. 5, we sum up the gap values of some Fe-based superconductors with different  $T_c$ , which were obtained from our point-contact spectroscopy measurements. The result of PrFeAsO<sub>0.89</sub>F<sub>0.11</sub> from NMR experiment [19] is also presented for comparison. It was noted that for all these Fe-based superconductors, the superconducting gaps can be divided into two groups with distinct energy scales centered at 4meV and 11meV, respectively. Recently, the Andreev reflection data suggested a gap of  $\Delta \approx 6.7\text{meV}$  for F-SmFeAsO with  $T_c = 42\text{K}$  and  $\Delta \approx 7\text{meV}$  with  $T_c = 45.5\text{K}$ . However, the isotropic *s*-wave gap was accepted in these analysis. If a *d*-wave gap was assumed, the obtained maximum gap  $\Delta_0$  is about 8meV, which should be ascribed to the big gap obtained in this work. Therefore, the high  $T_c$  can be achieved now is most possibly dominated by the big gap. However, the detailed gap structure is still an open issue until the high-quality single crystals can be obtained.

In summary, we have studied point-contact spectroscopy of the junctions built up between a normal-metal tip and the newly discovered Fe-based layered superconductor SmFeAsO<sub>0.9</sub>F<sub>0.1</sub>. A zero-bias conductance

peak was observed and demonstrated to be related to the surface Andreev bound states. Two superconducting gaps with different energy scales were observed which depend on the temperature in the similar way as predicted by BCS theory. Our data present strong evidence that SmFeAsO<sub>0.9</sub>F<sub>0.1</sub> is a nodal superconductor with multiple gaps.

We are grateful to Prof. Zhongxian Zhao and Dr. Zhian Ren for providing us the high quality SmFeAsO<sub>0.9</sub>F<sub>0.1</sub> samples made by high pressure technique. This work is supported by the Natural Science Foundation of China, the Ministry of Science and Technology of China ( 973 project No: 2006CB601000, 2006CB921802, 2006CB921300 ), and Chinese Academy of Sciences (Project ITSNEM).

\* Electronic address: lshan@aphy.iphy.ac.cn

† Electronic address: hhwen@aphy.iphy.ac.cn

- [1] Y. Kamihara et al., J. Am. Chem. Soc. **130**, 3296 (2008).
- [2] Z. A. Ren et al., Chin. Phys. Lett. **25**, 2215 (2008).
- [3] W. L. McMillan, Phys. Rev. **167**, 331 (1968).
- [4] H. H. Wen et al., EuroPhys. Lett. **82** (2008).
- [5] M. Rotter, M. Tegel, and D. Johrendt, arXiv:0805.4630.
- [6] G. Mu et al., arXiv:0803.0928.
- [7] L. Shan et al., arXiv:0803.2405.
- [8] C. Ren et al., arXiv:0804.1726.
- [9] K. Ahilan et al., arXiv:0804.4026.
- [10] Y. Nakai et al., arXiv:0804.4765.
- [11] H. Luetkens et al., arXiv:0804.3115.
- [12] Z. J. Yao, J. X. Li, and Z. D. Wang, arXiv:0804.4166.
- [13] T. Li, arXiv:0804.0536.
- [14] Q. Si and E. Abrahams, arXiv:0804.2480.
- [15] I. I. Mazin et al., arXiv:0803.2740.
- [16] K. Kuroki et al., arXiv:0803.3325.
- [17] T. Y. Chen et al., Nature (2008), doi:10.1038/nature07081.
- [18] K. A. Yates et al., arXiv:0806.0752.
- [19] K. Matano et al., arXiv:0806.0249.
- [20] J. Li and Y. P. Wang, Chin. Phys. Lett. **25**, 2232 (2008).
- [21] F. Marsiglio and J. E. Hirsch, arXiv:0804.0002.
- [22] Z. H. Wang et al., arXiv:0805.0736.
- [23] Q. Han, Y. Chen, and Z. D. Wang, EuroPhys. Lett. **82**, 37007 (2008).
- [24] S. Weyeneth et al., arXiv:0806.1024.
- [25] F. Hunte et al., Nature (2008), doi:10.1038/nature07058.
- [26] Z.-A. Ren et al., EuroPhys. Lett. **82** (2008).
- [27] L. Shan et al., Phys. Rev. B **68**, 144510 (2003).
- [28] G. Deutscher, Rev. Mod. Phys. **77**, 109 (2005), and references therein.
- [29] G. E. Blonder, M. Tinkham, and T. M. Klapwijk, Phys. Rev. B **25**, 4515 (1982).
- [30] S. Kashiwaya and Y. Tanaka, Rep. Prog. Phys. **63**, 1641 (2000).
- [31] M. Aprili et al., Phys. Rev. B **57**, R8139 (1998).
- [32] A. Plecenik et al., Phys. Rev. B **49**, 10016 (1994).
- [33] Y. Dagan, R. Krupke, and G. Deutscher, Phys. Rev. B **62**, 146 (2000).